Biophysical Chemistry 155 (2011) 10–19

Contents lists available at ScienceDirect

Biophysical Chemistry

journal homepage: http://www.elsevier.com/locate/biophyschem

Interaction of aristololactam-β-D-glucoside and daunomycin with poly(A): Spectroscopic and calorimetric studies

Abhi Das [a,1], Kakali Bhadra [a,1,2], Basudeb Achari [b], Prarthana Chakraborty [b], Gopinatha Suresh Kumar [a,*]

[a] Biophysical Chemistry Laboratory, Indian Institute of Chemical Biology, CSIR, Kolkata 700 032, India
[b] Chemistry Division, Indian Institute of Chemical Biology, CSIR, Kolkata 700 032, India

ARTICLE INFO

Article history:
Received 8 December 2010
Received in revised form 11 January 2011
Accepted 30 January 2011
Available online 16 February 2011

Keywords:
Aristololactam- β-D-glucoside
Daunomycin
Poly(A) binding
Isothermal titration calorimetry
Thermodynamic parameters

ABSTRACT

The binding of two sugar containing antibiotics viz. aristololactam-β-D-glucoside and daunomycin with single and double stranded poly(A) was investigated by spectroscopic and calorimetric studies. The binding affinity of daunomycin to ss poly(A) was of the order of $10^6\ M^{-1}$ and that to ds poly(A) was of the order of $10^5\ M^{-1}$. Aristololactam-β-D-glucoside showed a relatively weaker binding with an affinity of the order of $10^4\ M^{-1}$ with both the conformations of poly(A). Fluorescence studies showed maximum quenching for daunomycin-ss poly(A) complexes. The binding constants calculated from fluorescence spectroscopy were in good agreement with that obtained from UV spectroscopy. Moderate perturbation of circular dichroic spectra of both the conformations of poly(A) in presence of these molecules with concomitant formation of prominent extrinsic CD bands in the 300–450 nm region further revealed the association. Isothermal titration calorimetry results showed an overall entropy driven binding in all the four systems though the entropy change was maximum in daunomycin-ss poly(A) binding. The binding affinity was also maximum for daunomycin-ss poly(A) and varied as daunomycin-ds poly(A)> aristololactam-β-D-glucoside-ds poly(A)>aristololactam-β-D-glucoside-ss poly(A). A 1:1 binding stoichiometry was observed in all the cases, as confirmed by Job plot analysis, indicating the interaction to consist of a single binding mode. Ferrocyanide quenching studies showed good stacking interaction in all cases but was best for daunomycin-ss poly(A) interaction. No self-structure formation was observed in poly(A) with both daunomycin and aristololactam-β-D-glucoside suggesting the hindrance of the sugar moiety for such structural organization.

1. Introduction

New roles played by RNA in various crucial cellular processes is now getting unraveled and a new 'world of RNA' has emerged since the discovery of several new RNAs like mirco RNA, siRNA, ds RNA and many others in the cell with myriad structures and functions [1–6]. More importantly, the crucial new roles of many RNA molecules in the progression of parasites and viruses have resulted in their recognition as prime targets for therapeutic intervention. Consequently, in the last few years, there has been a paradigm shift to study and understand the fundamentals of small molecule interactions with various RNA structures in order to develop RNA targeted antibiotics for therapeutic use [7–9]. Rational design of RNA targeted drugs needs a detailed knowledge of the mode, mechanism, base specificity and structural selectivity data. DNA binding studies were pursued in a number of laboratories spanning the last 50 years and currently we have a robust understanding of the mode, mechanism, specificity, and energetics of binding [10–15]. However, such data in respect of RNA is virtually nonexistent except for some studies with aminoglycosides and alkaloids [8,16–21]. Since RNA, unlike DNA, folds to complex and diverse structures, generation of such fundamental data, both experimental and theoretical, needs extensive and painstaking study with each RNA structure. DNA binding molecules are good models to begin with for elucidating RNA binding aspects. Some RNA binding molecules like aminoglycosides have been investigated, but due to the high toxicity, their usage in RNA therapeutics is limited [22]. Our laboratory has studied the interaction of a number of natural alkaloid molecules and has provided new data on the mode, mechanism and energetics of their interaction with single and ds RNAs [23–28]. Poly(A) has been the focus of increasing attention for its importance in mRNA functioning [29,30]. All eukaryotic mRNAs have a long poly(A) tail at the 3′-end that is an important determinant in its maturation and stability and in the initiation of translation. Molecules that could bind to the polyadenylate tail were thought to inhibit mRNA and protein production in the cell. Post-transcriptional polyadenylation step in mRNA is catalyzed by the enzyme poly A polymerase (PAP). Many recent studies have implicated that neo PAP, a human PAP, was significantly over expressed in human cancer cells

* Corresponding author at: Biophysical Chemistry Laboratory, Indian Institute of Chemical Biology, CSIR, 4, Raja S.C. Mullick Road, Kolkata 700 032, India. Tel.: +91 33 2499 5723/2472 4049; fax: +91 33 2473 5197/2472 3967.
E-mail addresses: gskumar@iicb.res.in, gsk.iicb@gmail.com (G.S. Kumar).
[1] A.D. and K.B. contributed equally to this work.
[2] Current address: Department of Zoology, University of Kalyani, Kalyani, West Bengal 741 741 235, India.

0301-4622/$ – see front matter © 2011 Elsevier B.V. All rights reserved.
doi:10.1016/j.bpc.2011.01.011

in comparison to its expression in normal or virally transformed cells [31,32]. Therefore, it is likely that small molecules that bind to the poly(A) tail could interfere in the mRNA processing by PAP and may emerge as new type of RNA based therapeutic agents. It is also noteworthy that polyriboadenylic acid has the unique characteristic to exist in single stranded helical structure and parallel stranded double helix [33–35], the later being stabilized by base paired protonated adenines. Furthermore, many small molecules, particularly alkaloids, have been shown to induce unique self-structure in poly(A), the mechanism of which is still obscure [8,9,25,26,36,37]. Apparently, molecules that could induce self-structure in poly(A) may be useful as potential lead compounds for controlling the poly(A) chain elongation and mRNA degradation. In this context it may be noted that the possibility of double stranded poly(A) formation leading to arrest of protein production has not been ruled out [3,4]. To understand the molecular basis of self-structure formation, the binding aspects of more complex molecules to single and double stranded poly(A) needs to be investigated. Towards this goal, in this study we investigated the potential of two sugar bearing planar DNA binding antibiotics viz. aristololactam-β-D-glucoside and daunomycin (Fig. 1), to interact with single and double stranded poly(A) in order to understand the role of the sugar groups in self-structure induction.

2. Materials and methods

2.1. Materials

Polyriboadenylic acid [poly(A)] as potassium salt was purchased from Sigma-Aldrich Corporation (St. Louis, MO, USA) and used without further purification. Concentration of poly(A) in terms of nucleotide phosphate (hereafter nucleotide) was determined by UV absorbance measurements at 257 nm using a molar extinction coefficient (ε) value of 10,000 $M^{-1}\,cm^{-1}$ [38]. The expressed concentration refers to monomeric units of nucleotides in single stranded polynucleotide. Daunomycin (hereafter DAU) was obtained from Sigma-Aldrich Corporation and was used as received. Aristololactam-β-D-glucoside (hereafter ADG) was extracted from *Aristolochia indica* and crystallized from ethanol, and its purity was checked by various physicochemical techniques [39,40]. Buffer salts and other reagents were from Sigma-Aldrich.

2.2. Preparation and characterization of double stranded poly(A)

Poly(A) exists in the parallel stranded double strand conformation at or below pH 4.5 [33–35]. Double stranded poly(A) [hereafter ds poly(A)] was prepared by slowly adding single stranded poly(A) to buffer of pH 4.5 under stirring. At least 2 h time was allowed for the transition to be complete and the same was monitored by absorption and circular dichroism studies. The absorption maximum of ss poly(A) was at 257 nm that blue shifted by 5 nm on conversion to ds structure, accompanied by a hypochromic effect of about 15%. The circular dichroic spectrum of ss poly(A) has a positive band with maximum around 265 nm followed by a negative band around 248 nm with a hump around 210 nm. Double stranded conformation of poly(A), on the other hand, has a strong band around 263 nm followed by a weak negative band around 242 nm. Double stranded poly(A) structure was characterized by cooperative optical melting in UV and CD with a melting temperature of 83 ± 1 °C compared to a broad absorption change for the ss poly(A). The comparative characteristics of ss and ds poly(A) are presented in Fig. 2.

2.3. Preparation of ADG and DAU solutions

Stock solutions of ADG and DAU were prepared in the respective experimental buffers and kept protected in the dark. Both compounds obeyed Beer's law in the concentration range used in this study. The concentration of DAU and ADG were determined by absorbance measurements using molar extinction coefficients (ε) as follows: DAU-11,500 $M^{-1}\,cm^{-1}$ at 480, and ADG-10,930 $M^{-1}\,cm^{-1}$ at 398 nm (in DMSO), respectively. Experiments were performed in 20 mM citrate-phosphate (CP) buffer with ss poly(A) of pH 7.2 and 50 mM CP buffer of pH 4.5with ds poly(A). For ADG binding studies the buffer contained additionally 240 mM of DMSO.

2.4. Absorption titration experiments

The absorption spectral titrations were performed under stirring at 20 ± 0.5 °C on a Jasco V660 unit (Jasco International Co. Ltd., Tokyo, Japan) equipped with a thermoelectrically controlled cell holder and temperature controller in matched quartz cells of 1 cm path length, following generally the methods standardized in our laboratory and described earlier [25,26,41].

2.5. Analysis of binding data and evaluation of binding parameters

The spectral changes observed in absorption measurements were used to calculate the intrinsic binding constants using Scatchard plots of r/C_f versus r that were further analyzed using the neighbor exclusion model of McGhee–von Hippel [42],

$$r / C_f = K_i(1-nr)[(1-nr)/\{1-(n-1)r\}]^{(n-1)} \quad (1)$$

where r is the molar ratio of the bound ligand to polynucleotide, C_f is the free ligand concentration, K_i is the intrinsic binding constant to an isolated binding site, and n is the exclusion parameter. All the binding data were analyzed using Origin 7.0 software (Origin Labs, Northampton, MA, USA) to determine the best-fit parameters of K_i and n. The spectral data were also analyzed by constructing Benesi–Hildebrand plots [43] using the following relation,

$$1 / \Delta A = 1 / \Delta A_{max} + 1 / K_{BH}(\Delta A_{max})x1 / [M] \quad (2)$$

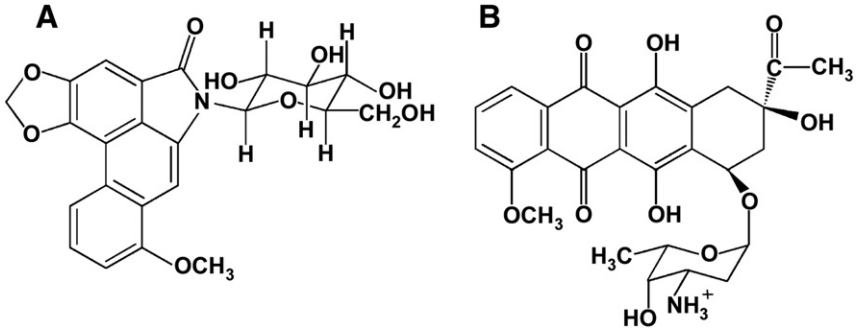

Fig. 1. Chemical structure of (A) aristololactam–β-D-glucoside and (B) daunomycin.

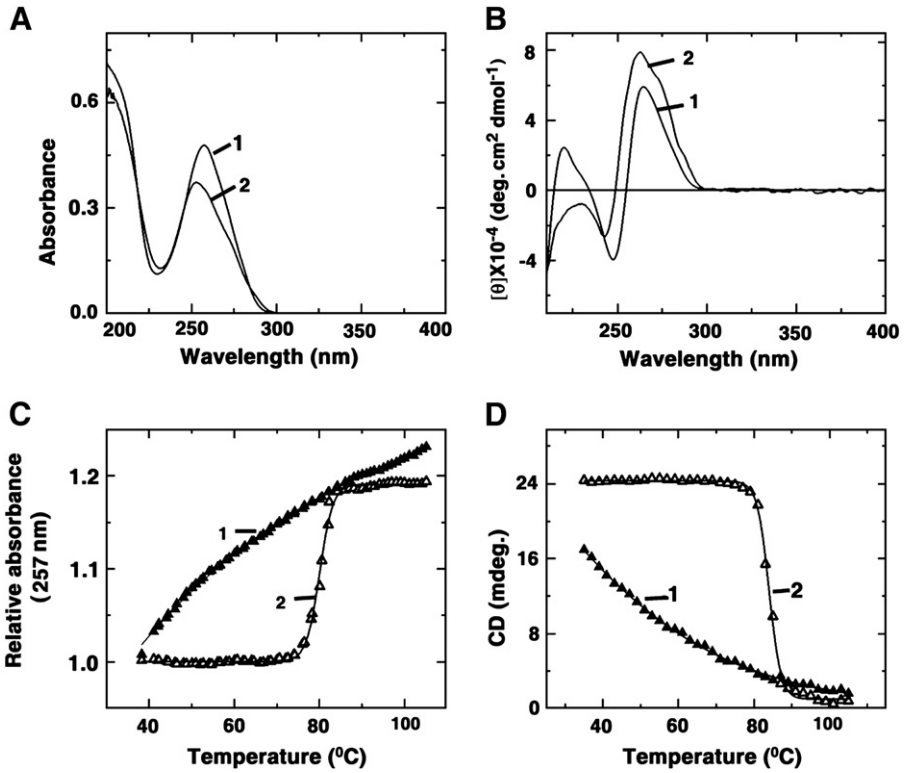

Fig. 2. (A) Absorption spectra (50 μM), (B) CD spectra (80 μM) (C) UV melting profiles (50 μM), and (D) CD melting profiles (80 μM) of single (curve 1) and double stranded (curve 2) poly(A). Buffer conditions: citrate phosphate buffer, 20 mM [Na^+], pH 7.2 and 50 mM [Na^+], pH 4.5, for ss poly(A) and ds poly(A), respectively.

where ΔA is the change in absorbance at a given wavelength and [M] is the concentration of poly(A). By plotting the reciprocal of the absorbance intensity with respect to reciprocal concentration of poly(A), the Benesi–Hildebrand association constant for the complex formation (K_{BH}) was calculated from the ratio of the slope to the intercept [43,44].

2.6. Fluorescence studies

Steady state fluorescence measurements were performed on a Hitchi-F4010 fluorescence spectrometer (Hitachi, Tokyo, Japan) in fluorescence-free quartz cuvettes of 1 cm path length as described previously [45]. The excitation wavelengths for ADG and DAU were 400 and 480 nm, respectively. Fluorescence emission intensity was monitored at 485 nm for ADG and 555 nm for DAU, keeping an excitation and emission band pass of 5 nm. The sample cell was thermostated using an Eyela Unicool water bath (Tokyo Rikakikai, Tokyo, Japan) and all the measurements were performed at 20 ± 0.5 °C under conditions of constant stirring. Uncorrected fluorescence spectra were recorded. Quenching experiments were performed as described earlier [19].

2.7. Continuous variation analysis (Job's plot)

Job's continuous variation method was employed to determine the binding stoichiometry by fluorescence spectroscopy [46–48]. At constant temperature, the fluorescence signal was monitored for solutions where the concentrations of both poly(A) and the drug were varied while the sum of their concentrations was kept constant at 50 μM. The difference in fluorescence intensity (ΔF) of the drugs in the absence and presence of poly(A) was plotted as a function of the input mole fraction of each drug as reported previously [48,49]. The break point in the resulting plot corresponds to the mole fraction of the bound drug in the complex. The stoichiometry was obtained in terms of poly(A)-drug[$(1-\chi_{drug})/\chi_{drug}$] where χ_{drug} denotes the mole fraction of the respective drug. The results presented are averages of at least three experiments.

2.8. Circular dichroic spectropolarimetry

Circular dichroic (CD) spectra were recorded on a PC controlled Jasco J815 unit (Jasco International Co. Ltd.,) equipped with a temperature controller and thermal programmer model PFD 425 L/15 in rectangular quartz cuvettes of 1 cm path length at 20 ± 0.5 °C as reported earlier [50]. Each spectrum was averaged from at least five successive scans at a scan rate of 100 nm/min. using a band width of 1 nm at a sensitivity of 100 millidegree, and was base line corrected and smoothed within permissible limits using the built-in Jasco software. CD melting profiles were obtained by heating the sample (55.0 μM of poly(A) and 13.5 μM of each drug) at a scan rate of 0.8 °C/min and monitoring the CD signal at 274 nm [25]. For the melting profiles, the ellipticity values are expressed in units of millidegrees. All CD measurements were repeated at least three times and the data are the average of these determinations.

2.9. Thermal melting studies

Absorbance versus temperature profiles (optical melting curves) of the complexes were measured on a Shimadzu Pharmaspec 1700 spectrophotometer equipped with a peltier controlled TMSPC-8 model microcell accessory (Shimadzu Corporation, Kyoto, Japan), as reported previously [51]. In a typical melting experiment, poly(A) samples were mixed with the respective drug under investigation and diluted into the desired degassed buffer in the micro optical eight chambered cuvette of 1 cm light path length. The temperature of the microcell accessory was raised at a heating rate of 0.5 °C/min. continuously monitoring the absorbance change at 257 nm. Melting curves allowed the monitoring of the hyperchromic change and estimation of melting temperature, T_m, the midpoint of the hyperchromic transition.

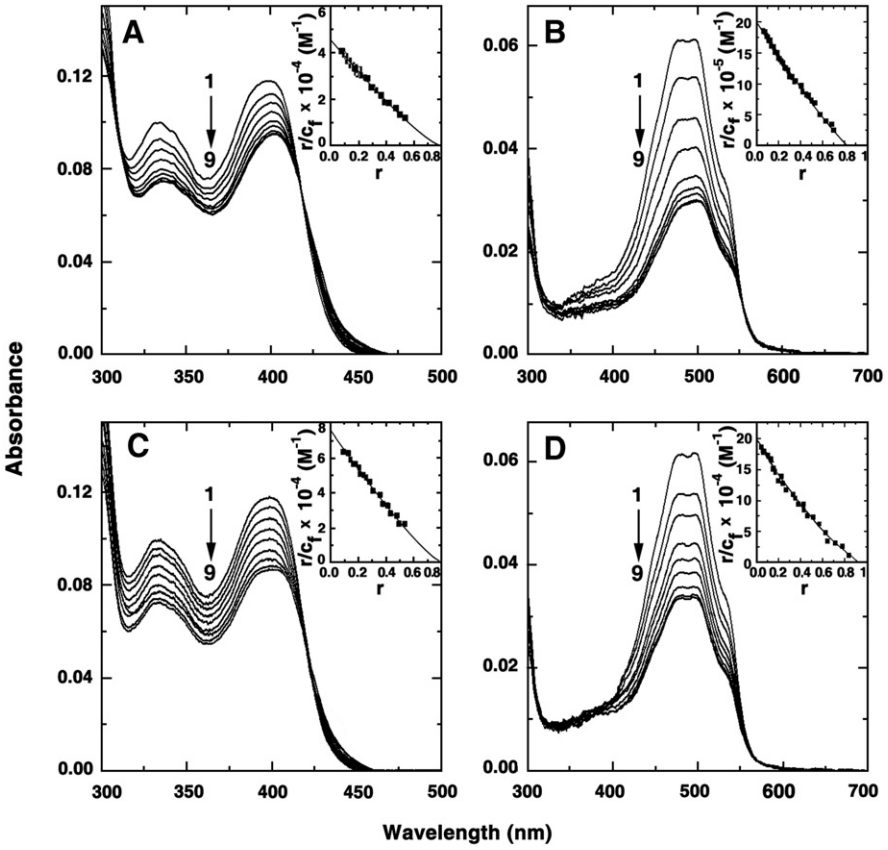

Fig. 3. Absorption spectral titration of (A) ADG (10.8 μM) treated with 108, 216, 324, 432, 540, 756, 972, 1296 and 1620 μM (curves 1–9) of ss poly(A), (B) DAU (5.3 μM) treated with 10.6, 21.1, 31.8, 42.4, 53.0, 63.6, 84.8, 106.0 and 127.2 μM (curves 1–9) of ss poly(A), (C) ADG (10.7 μM) treated with 107, 214, 321, 428, 535, 749, 1070, 1605 and 2140 μM (curves 1–9) of ds poly(A) and (D) DAU (5.3 μM) treated with 10.6, 21.1, 31.8, 53.0, 79.5, 106, 132.5, 159.0 and 185.5 μM (curves 1–9) of ds poly(A), respectively. Inset: representative Scatchard plot of each complexation. The solid lines represent the non-linear least square best fit of the experimental points to the neighbor exclusion model. All experiments were performed at 20 ± 0.5 °C in CP buffer, 20 mM [Na^+], pH 7.2 for ss poly(A) and CP buffer, 50 mM [Na^+], pH 4.5 for ds poly(A).Values of K_i (intrinsic binding constant) are presented in Table 2.

2.10. Isothermal titration calorimetry

All isothermal titration calorimetry experiments were performed using a MicroCal VP-ITC unit (MicroCal, Inc., Northampton, MA, USA) at 20 °C as reported previously [49,50]. Aliquots of degassed poly(A) solution were injected from a rotating syringe (290 rpm) into the isothermal sample chamber containing each of the drug solutions [1.4235 mL, 50 μM DAU and 200 μM ADG, respectively, for ss poly(A) and 250 μM of ADG and DAU for ds poly(A)]. Corresponding control experiments to determine the heat of dilution of poly(A) were performed by injecting identical volumes of the same concentration of poly(A) into the buffer. The duration of each injection was 10 s and the delay time between each injection was 240 s. The initial delay before the first injection was 60 s. Each injection generated a heat burst curve (microcalories per second versus time). The area under each heat burst curve was determined by integration using the Origin 7.0 software (MicroCal) to give the measure of the heat associated with that injection. The heat associated with each poly(A)-buffer mixing was subtracted from the corresponding heat associated with the poly(A) injection to the drug to give the heat of drug binding to poly(A). The heat of dilution of injecting the buffer into each of the drug solution was observed to be negligible. The resulting corrected injection heats were plotted as a function of the D/P [drug]/nucleotide phosphate molar ratio, fit with a model for one set of binding sites, and analyzed using Origin 7.0 software to estimate the binding affinity (K), the binding stoichiometry (N) and the enthalpy of binding (ΔH). The Gibbs energies (ΔG) were calculated using the standard relationship

$$\Delta G = -RT\ln(K) \tag{3}$$

where R is the gas constant (1.987 cal K^{-1} mol^{-1}) and T is the temperature in Kelvin (293 K).

The binding free energy coupled with the binding enthalpy derived from the ITC data allowed the calculation of the entropic contribution to the binding ($T\Delta S$), where ΔS is the calculated binding entropy using the standard relationship.

$$T\Delta S = \Delta H - \Delta G \tag{4}$$

Table 1
Summary of optical properties of free and bound drugs.

Parameter	ss poly(A)		ds poly(A)	
	ADG	DAU	ADG	DAU
Absorbance				
λ_{max} (free)	398	480	398	480
λ_{max} (bound)	401	496	400	480
λ_{iso}[a]	418	–	422	–
ε_f (at λ_{max})	10,930	11,500	10,930	11,500
ε_b(at λ_{max})	8680	5390	8180	6310
ε_{iso} (at λi_{so})	6482 (418)	–	5047 (422)	–
Fluorescence				
λ_{max} (excitation)	400	480	400	480
λ_{max} (emission)	485	555	485	555
F_b/F_o[b]	0.86	0.35	0.82	0.74

Units: λ nm; ε (molar extinction coefficient) M^{-1} cm^{-1}.
[a] Wavelength at the isosbestic points.
[b] F_o and F_b are the fluorescence intensities of the free and completely bound drug at 485 and 555 nm in case of ADG and DAU, respectively.

Table 2
Binding constant from spectroscopic data.

Poly(A) conformation	Spectrophotometry				Spectrofluorimerty (ferrocyanide quenching)			
	Scatchard analysis		BH plot		ADG		DAU	
	ADG	DAU	ADG	DAU	K_{sv} L mol^{-1}			
	$K_i \times 10^{-4}$ (M^{-1})	$K_i \times 10^{-5}$ (M^{-1})	$K_{BH} \times 10^{-5}$ (M^{-1})	$K_{BH} \times 10^{-6}$ (M^{-1})	Free	Bound	Free	Bound
Single strand	4.50	19.9	4.58	2.08	61.2	53.8	117.6	78.7
Double strand	7.54	1.98	6.13	0.11	61.2	57.8	117.6	83.1

Average of four determinations at 20 ± 0.5 °C in CP buffer of 20 mM [Na^+], pH 7.2 for ss poly(A) and 50 mM [Na^+], pH 4.5 for ds poly(A). Binding constants (K_i) refer to values obtained from Scatchard plots through McGhee–von Hippel analysis.

3. Results and discussion

3.1. Spectrophotometric results and evaluation of binding affinity

In the absorption region 300–600 nm, both ADG and DAU have characteristic absorption spectra. The changes in the absorption spectra may be conveniently used to monitor the interaction with poly(A). In Fig. 3A–D, absorption spectral changes in ADG and DAU on titration with increasing concentration of single and double stranded poly(A) are presented. The spectrum marked '1' is the absorption spectrum of the free drug molecule in each case. All the absorption spectral titrations showed hypochromic and bathochromic effects. Titration of ss poly(A) with ADG (Fig. 3A) showed gradual hypochromic change at 398 nm with increasing P/D (nucleotide phosphate/drug molar ratio) and a slight bathochromic shift of 2–3 nm with an isosbestic point at 418 nm. At saturating P/D, the change in hypochromicity was about 21%. On the other hand, DAU-ss poly(A) showed large hypochromic effect at 480 nm with a bathochromic effect of about 15 nm (Fig. 3B). The hypochromicity change at saturation was about 53% in this case. Absorption spectral titration of the binding of ADG and DAU with ds poly(A) is presented in Fig. 3C and D. In both cases, hypochromic effects were observed at the respective wavelength maximum with bathochromic shifts. The hypochromic change was more pronounced in case of ADG-ds poly(A) complexation compared to ss poly(A), while ss poly(A) titration registered more changes compared to the ds poly(A) for DAU. Hypochromic changes with bathochromic shifts generally occur due to stacking/intercalative interaction of the ligand molecules with the base/base pairs of the nucleic acid. The optical properties of free and poly(A) bound ADG and DAU molecules are presented in Table 1.

The results of the spectrophotometric titration data were expressed as Scatchard plots and analyzed further by the McGhee–von Hippel methodology [42] for non cooperative binding for evaluation of the binding constants The Scatchard plots are depicted in the inset of Fig. 3. The binding affinity of ADG and DAU to ss poly(A) were evaluated as 4.50×10^4 M^{-1} and 1.99×10^6 M^{-1}, respectively. For ds

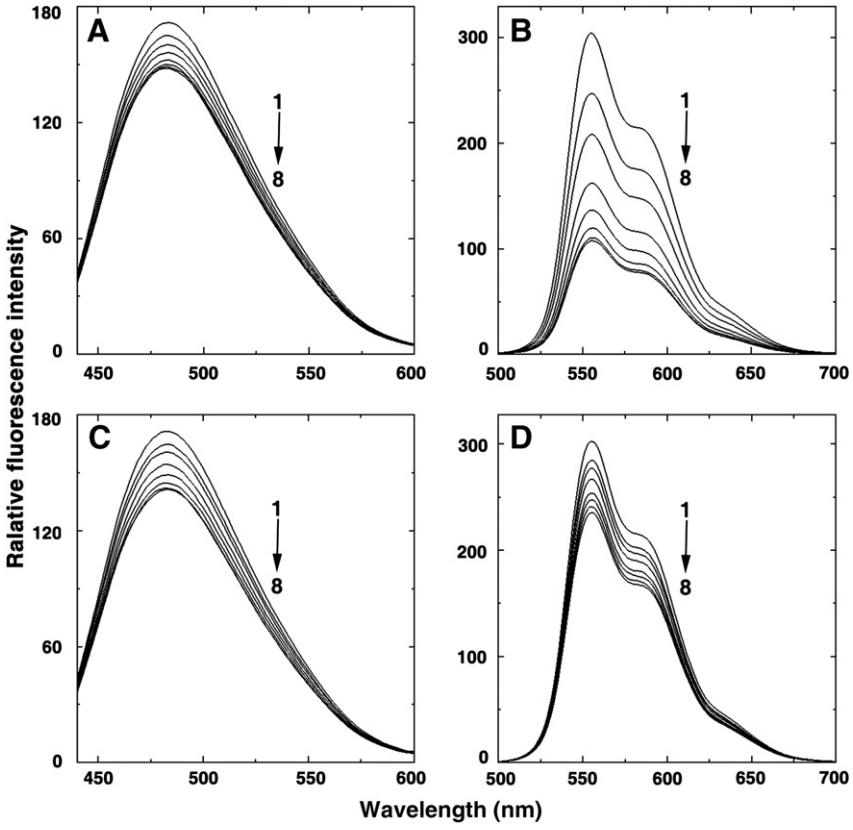

Fig. 4. Representative fluorescence spectra of (A) ADG (3.07 μM) treated with 30.7, 61.4, 122.8, 184.7, 245.6, 307, 460.5 and 614.0 μM (curves 1–8) of ss poly(A), (B) DAU (5.0 μM) treated with 10, 20, 30, 50, 75, 100, 125, and 150 μM (curves 1–8) of ss poly(A), (C) ADG (3.07 μM) treated with 30.7, 61.4, 122.8, 184.7, 245.6, 307.0, 460.5 and 614.0 μM (curves 1–8) of ds poly(A), (D) DAU (5.0 μM) treated with 20, 40, 60, 80, 100, 125, 150 and 200 μM (curves 1–8) of ds poly(A), respectively. Experiments were performed at 20 ± 0.5 °C in CP buffer, 20 mM [Na^+], pH 7.2 for ss poly (A) and CP buffer, 50 mM [Na^+], pH 4.5 for ds poly(A).

poly(A), the affinity values of ADG and DAU were $7.54\times10^4\ M^{-1}$ and $1.98\times10^5\ M^{-1}$, respectively. The number of binding sites obtained were 1.25 and 1.24 for ADG and 1.19 and 1.09 for DAU-ss and ds poly(A) complexation. We also analyzed the spectral change data by the Benesi–Hildebrand protocol [43,44]. The ratio of the intercept to the slope gave K_{BH}, the apparent binding constant. From this analysis, it was found that the binding affinity values of ADG and DAU to ss poly(A) were $4.58\times10^4\ M^{-1}$ and $2.08\times10^6\ M^{-1}$, respectively, and that to ds poly(A) were $6.13\times10^4\ M^{-1}$ and $1.10\times10^5\ M^{-1}$. These values are presented in Table 2. The values of the affinity obtained from this analysis were in excellent agreement with each other. The binding affinity of DAU to ss poly (A) was the highest, of the order of $10^6\ M^{-1}$, and the binding affinity values of ADG to both ss and ds poly(A) were weaker compared to those with DAU. It is worth noting that DAU has a perfectly intercalating anthaquinone chromophore and additional H-bonding anchor and a phosphate/groove binding daunosamine moiety while ADG has only an intercalating chromophore with a neutral sugar molecule. The differences in the functional domains of the two molecules may be responsible for the large differences in the binding affinity.

3.2. Fluorescence spectroscopic studies

ADG and DAU are strong fluorescent molecules. Their emission spectra are in the 440–600 and 500–700 nm regions, respectively, with maxima around 485 and 555 nm when excited around 400 and 480 nm, respectively. Complex formation was monitored by titration studies keeping a constant concentration of the drug and increasing the concentration of poly(A). With increasing concentration of both single and double stranded poly(A), progressive quenching of the fluorescence was observed for both ADG and DAU eventually reaching the saturation point without any shift in the wavelength maximum (Fig. 4A–D). But the extent of quenching was significantly different in each case. Maximum fluorescence quenching (65%) was observed with DAU-ss poly(A) (Fig. 4B) indicating possibly a strong association of the DAU molecule to the ss poly(A) where as quenching of ADG with ss poly(A) (Fig. 4A) was comparatively lower at about 15%. The percentage of quenching of ADG and DAU interaction (Fig. 4C,D) with ds poly(A) was about 18 and 26%, respectively. Thus, the fluorescence titration studies indicated that maximum quenching was observed for DAU-ss poly(A) and in other cases it followed as DAU-ds>ADG-ds>ADG-ss poly(A). This trend is similar to the binding affinity revealed from the absorption spectral study (Fig. 3 and Table 2).

The stoichiometry of the association was determined independently by continuous variation analysis (Job's plot) in fluorescence [46,47]. The plot of the difference in fluorescence intensity (ΔF) at 485 nm and 555 nm for ADG and DAU, respectively, versus their mole fractions (Fig. 1, ESI) revealed a single binding mode for both ligands on both ss and ds poly(A). From the inflection point, $X_{\text{ADG-ss poly(A)}}=0.45$ ($n=1.20$ np), $X_{\text{DAU-ss poly(A)}}=0.45$ ($n=1.20$ np), $X_{\text{ADG-ds poly(A)}}=0.44$ ($n=1.24$ np) and $X_{\text{DAU-ds poly(A)}}=0.48$ ($n=1.08$ np) were estimated.

3.3. Circular dichroic studies

Conformational changes associated with the binding of ADG and DAU with ss and ds poly(A) were probed through circular dichroic studies. Single stranded poly(A) has a characteristic CD spectrum with a large positive band around 265 nm and a less intense negative band around 248 nm (curve 1 in Fig. 5A, B). CD spectral changes accompanying the interaction of ADG with ss poly(A) were characterized by a small decrease in the positive peak at 265 nm with concomitant decrease in the negative CD ellipticity. The formation of a broad negative induced CD band in the 300–400 nm region whose ellipticity enhanced as the binding progressed,

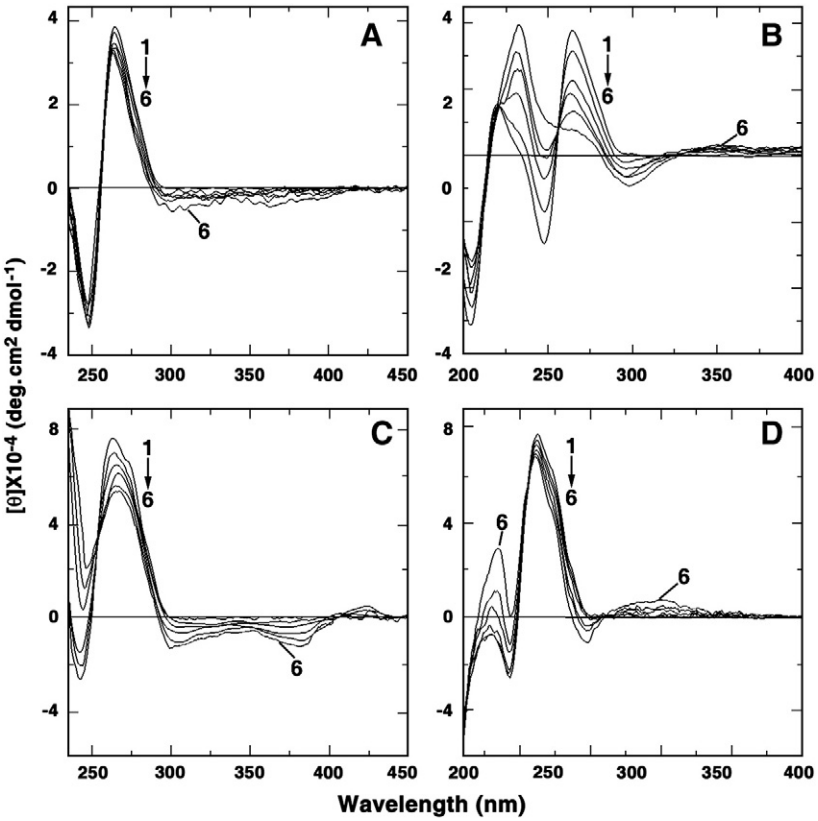

Fig. 5. Circular dichroic spectra of ss poly(A) (40 μM) treated with (A) 20, 40, 60, 80, 100 and 120 μM (curves 1–6) of ADG, (B) ss poly(A) (40 μM) treated with 8, 16, 24, 40, 60 and 80 μM (curves 1–6) of DAU, (C) ds poly(A) (40 μM) treated with 20, 40, 60, 80, 100 and 120 μM (curve 1–6) of ADG and (D) ds poly(A) (40 μM) treated with 8, 16, 24, 40, 60 and 80 μM (curve 1–6) of DAU, respectively. Experiments were performed at 20 ± 0.5 °C in CP buffer, 20 mM [Na^+], pH 7.2 for ss poly(A) and CP buffer, 50 mM [Na^+], pH 4.5 for ds poly(A).

is also visible (Fig. 5A–D). Interaction of DAU with ss poly(A) also showed decrease in the positive peak at 265 nm and the negative 250 nm band but the change in ellipticity was much more pronounced; the negative band at 250 nm showed reduction in ellipticity, crossing over to the positive side at the saturation. Concomitant with the intrinsic CD changes, the formation of a weak and broad positive extrinsic CD band in the 300–400 nm region was evident. The decrease in ellipticity of the 265 nm band for ds poly(A) complexation with ADG was more pronounced with the negative 250 nm CD band crossing over to the positive side. The formation of a negative induced CD band in the 300–400 nm region was seen. The binding of ADG to the ss poly(A) showed small decrease in ellipticity of the long wavelength band. Thus, the CD changes revealed that ss and ds poly (A) bind differently with the two drugs depending on their functional groups. These results may be used to establish a method for distinguishing among the binding modes.

3.4. Fluorescence quenching studies

Fluorescence quenching experiments provide an effective method for investigating the binding of small molecules to nucleic acid structure [52]. In the complex, molecules that are free or bound on the surface of the poly(A) may be readily available to an anionic quencher, while those bound inside may be shielded. The electrostatic barrier due to the negative charges on the phosphate groups at the helix surface limits the penetration of an anionic quencher into the helix. Hence, very little or no quenching may be observed in the presence of an anionic quencher, if the binding involves stacking interactions. Consequently the magnitude of the Stern–Volmer quenching constant (K_{sv}) of the ligands that are bound inside will be lower than that of the free molecules. It has been revealed that binding to poly(A) resulted in somewhat decreased quenching of the fluorescence intensity of ADG and DAU (Fig. 2, ESI). K_{sv} values (Table 2) for free ADG and its complexes with the ss poly(A) and ds poly(A) were 61.2, 53.8 and 57.8 L/mol, respectively, while the same for DAU were 117.6, 78.0 and 83.0 L/mol. This indicated that the binding of DAU to both ss and ds poly(A) hindered to some extent the accessibility of the quencher to the bound ligand molecules suggesting deep stacking of DAU to the polynucleotide, or in other words bound ligand molecules are considerably protected and sequestered away from the solvent suggesting strong binding with poly(A).

3.5. Isothermal titration calorimetry

To characterize the energetics of binding, isothermal titration calorimetry was used. ITC is an important and reliable tool for the direct measurement of thermodynamic parameters in various biological interactions [53–55]. In Fig. 6 A–D (upper panels) the representative raw ITC profiles resulting from the titration of ss and ds poly(A) to ADG and DAU solutions are presented. Each of the heat burst curve in the figure corresponds to a single injection. The areas under these heat burst curves were determined by integration to yield the associated injection heats. These injection heats were corrected by subtracting the corresponding dilution heats derived from the injection of identical amounts of the injectant, poly(A), into the buffer alone. In the lower panel of the figure, the resulting corrected injection heats are plotted against the respective molar ratios. In this panel the data points reflect the experimental injection heat while the solid lines reflect calculated fits of data. The corrected isotherms obtained at 20 °C showed single site binding in all the cases indicating that one type of complexation is formed exclusively, thus enabling the fitting to a single site protocol in ITC. The binding affinity and the other thermodynamic parameters of ADG and DAU to ss and ds poly(A) are presented in Table 3. The data showed an overall entropy driven binding in all the four cases though the entropy contribution to the Gibbs energy change was maximum in DAU-ss poly(A) binding. The Gibbs energy change in each system was more or less similar in the range of ~6.3–7.0 kcal/mol except in case of DAU-ss poly(A) where ΔG was −8.47 kcal/mol. The ITC data of ADG-ss poly(A) (Fig. 6A) complexation yielded a K value of $5.7\times10^4\ M^{-1}$, a small enthalpy change (ΔH) of −0.82 kcal/mol, and an entropy change ($T\Delta S$) of 5.57 kcal/mol. The binding with DAU-ss poly(A) (Fig. 6B) on the other hand yielded a higher K value of $2.03\times10^6\ M^{-1}$, a ΔH of −2.09 kcal/mol and a large entropy change of 6.39 kcal/mol. Further, in case of interaction with ADG-ds poly(A) (Fig. 6C), the binding affinity was $8.43\times10^4\ M^{-1}$, while an enthalpy change of −2.70 kcal/mol and an entropy change of

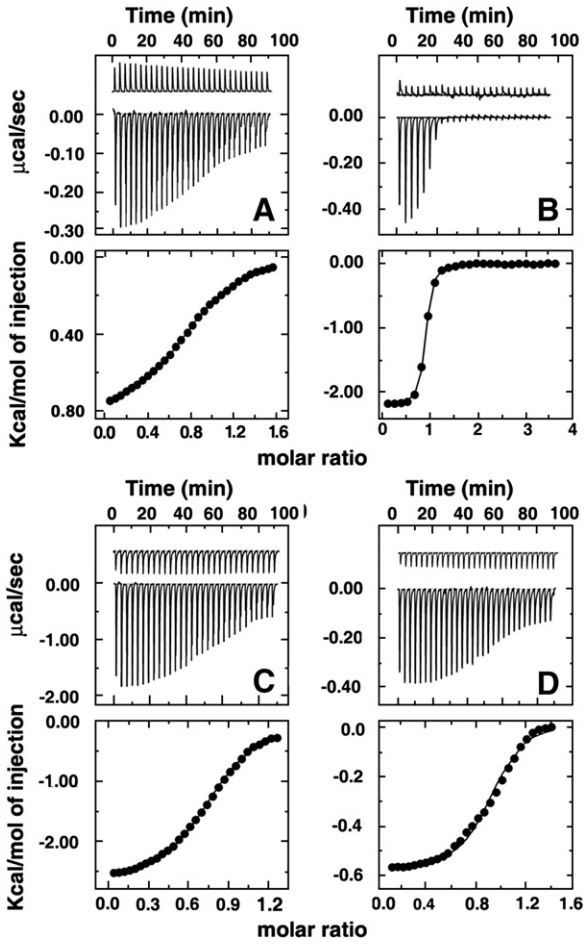

Fig. 6. ITC profiles for the binding of (A) ADG with ss poly(A) (B) DAU with ss poly(A) (C) ADG with ds poly(A) and (D) DAU with ds poly(A). The top panels represent the raw data for sequential injection of drug into poly(A) solution and the bottom panels show the integrated heat data after correction of heat of dilution against molar ratio of poly(A)/drug. The data points (closed circle) were fitted to a one site model, and the solid lines represent the best fit data. Experiments were performed at 20 ± 0.5 °C in CP buffer, 20 mM [Na^+], pH 7.2 for ss poly(A) and CP buffer, 50 mM [Na^+], pH 4.5 for ds poly(A).

Table 3
Thermodynamic parameters of the binding of ADG and DAU to poly(A) at 20 °C.

Poly(A) conformation	Drug	$K\times10^{-5}$ (M^{-1})	N	ΔH (kcal/mol)	$T\Delta S$ (kcal/mol)	ΔG (kcal/mol)
Single strand	ADG	0.57	1.23	−0.82	5.57	−6.38
	DAU	20.3	1.22	−2.09	6.39	−8.47
Double strand	ADG	0.84	1.28	−2.70	3.90	−6.60
	DAU	2.14	1.11	−0.53	6.62	−7.15

Data in this table are derived from ITC experiments and average of four determinations. Single strand poly(A) binding experiments were conducted in citrate–phosphate buffer of 20 mM [Na^+], pH 7.2.Double strand poly(A) binding experiments were conducted in citrate-phosphate buffer of 50 mM [Na^+], pH 4.5. K and ΔH values were determined from ITC profiles fitting to Origin 7.0 software as described in the text. The values of ΔG and $T\Delta S$ were determined using equations $\Delta G = -RT\ln K$, and $T\Delta S = \Delta H - \Delta G$. All ITC profiles were fit to a model of single binding sites.

Table 4
Thermodynamic parameters for the binding of ADG and DAU to ss poly(A) in four different [Na^+] concentrations.

Drug	NaCl (mM)	$K\times10^{-5}$ (M^{-1})	N	ΔG (kcal/mol)	ΔH (kcal/mol)	$T\Delta S$ (kcal/mol)	ΔG_t (kcal/mol)	ΔG_{pe} (kcal/mol)
ADG	10	0.68	1.17	−6.48	−2.71	3.78	−5.56	−0.96
	20	0.57	1.23	−6.38	−0.82	5.57	−5.60	−0.82
	30	0.47	1.23	−6.28	−0.68	5.60	−5.57	−0.73
	50	0.39	1.26	−6.16	−0.51	5.65	−5.56	−0.62
DAU	10	33.1	1.13	−8.75	−2.48	6.27	−7.13	−1.67
	20	20.3	1.22	−8.47	−2.08	6.39	−7.09	−1.42
	30	14.2	1.30	−8.24	−1.68	6.56	−7.02	−1.28
	50	12.1	1.50	−8.15	−1.23	6.91	−7.12	−1.09

Data in this table are derived from ITC experiments conducted in citrate–phosphate buffer of different [Na^+], pH 7.2 and are averages of four determinations. K and ΔH values were determined from ITC profiles fitting to Origin 7.0 software as described in the text. The values of ΔG and $T\Delta S$ were determined using equations $\Delta G = -RT\ln K$, and $T\Delta S = \Delta H - \Delta G$. All ITC profiles were fit to a model of single binding sites.

3.90 kcal/mol were obtained. Binding of DAU-ds poly(A) on the other hand showed (Fig. 6D) a binding affinity of 2.14×10^5 M^{-1}, an enthalpy change of −0.53 kcal/mol and an entropy change of 6.62 kcal/mol. The binding affinity values at 20 °C evaluated from the ITC data (Table 3) are in good agreement with those evaluated from the spectroscopic data (Table 2). The binding was exothermic and the stoichiometry was found to be 1 mol of ligand binding per mol of poly(A) in all the cases. These values are in good agreement with the values obtained from Scatchard and Job plot analysis. It may be noted that DAU-ss poly(A) complex has the highest binding affinity in agreement with that revealed from spectroscopic experiments.

3.6. Salt dependent ITC studies: role of electrostatic interaction

DAU has a positive charge on its daunosamine sugar moiety [56]. ADG is apparently uncharged, but in presence of nucleic acids the formation of a weak positive charge at the N6 position has been proposed [57]. An ion pair formation between the quaternary N6 of ADG and phosphate oxygen of nucleic acids appears to be the driving force in its interaction. To understand the role of electrostatic interaction in the binding process, salt dependence of the binding of ADG and DAU with ss poly(A) at four [Na^+] concentrations viz, 10, 20, 30 and 50 mM was studied by ITC experiments. The results are presented in Table 4. The binding constant moderately decreased as the salt concentration increased and the plot of ln K versus ln [Na^+] gave straight lines in both cases (Fig. 3, ESI) with slopes of −0.36 and −0.62 equivalent to the number of sodium ions released. The number of ions released in case of DAU is in agreement with its single positive charge and the result of ADG study reveals the presence of a weak positive charge in the molecule. For double stranded DNA, it has been reported that ADG releases about 0.49 units of monovalent ions [57]. At all salt concentrations studied the binding was exothermic showing single mode of binding for both compounds.

The thermodynamic parameters elucidated from the ITC analysis are presented in Table 4. The binding affinity decreased only by 40% in ADG while there was a drop of about 65% in the case of DAU indicating a stronger role of the electrostatic interaction for the complexation of the latter. For both ADG and DAU, the enthalpy contribution to the Gibbs energy of the binding decreased and the entropy contribution increased; the change was much larger for ADG compared to DAU (Table 4). The parsing of the contribution to the Gibbs energy in terms of polyelectrolyte and non-polyelectrolyte forces indicated that the polyelectrolyte contribution to the binding free energy was significantly smaller in both cases but the same was higher for DAU compared to ADG (Fig. 4, ESI). In both cases the non-polyelectrolytic contribution remained invariant with the salt concentration. Thus, the major contribution to the binding free energy comes from forces other than the electrostatic interactions. This is in agreement with previous reports [58–60].

3.7. Temperature dependent ITC studies: heat capacity changes

We also studied the temperature dependence of the binding of ADG and DAU to ss-poly(A) from ITC experiments at four temperatures, viz. 10, 15, 20 and 30 °C. The thermodynamic parameters at these temperatures are presented in Table 5. It can be seen that the binding constant was reduced to half on raising the temperature from 10 to 30 °C for ADG complexation, while for DAU a larger variation was observed. The enthalpy values decreased (became more negative in both cases) but was compensated by smaller entropy contribution to keep the free energy change more or less constant (Fig. 7A). From the plots of the variation of the thermodynamic parameters with temperature, the heat capacity change was deduced to be around −40.16 and −70.65 cal/(mol K), respectively, for ADG and DAU binding to ss poly(A) (Fig. 7B). The heat capacity values are negative which indicated the involvement of significant hydrophobic contribution in the binding reaction in agreement with the salt dependence studies.

Table 5
Thermodynamic parameters for the binding of ADG and DAU to ss poly(A) in CP buffer (20 mM [Na^+]) pH = 7.2 at different temperatures.

Drug	Temperature (K)	$K\times10^{-5}$ (M^{-1})	N	ΔG (kcal/mol)	ΔH (kcal/mol)	$T\Delta S$ (kcal/mol)	ΔCp (cal/mol K)
ADG	283	0.68	1.09	−6.27	−0.44	5.83	
	288	0.62	1.15	−6.35	−0.60	5.75	−40.16
	293	0.57	1.23	−6.38	−0.82	5.57	
	303	0.35	1.25	−6.33	−1.24	5.09	
DAU	283	36.9	1.10	−8.50	−1.40	7.10	
	288	27.0	1.13	−8.53	−1.80	6.73	−70.65
	293	20.3	1.22	−8.47	−2.08	6.39	
	303	11.4	1.42	−8.39	−2.81	5.58	

The data in this table are derived from ITC experiments and are averages of four determinations. K and ΔH values were determined from ITC profiles fitting to Origin 7.0 software as described in the text. The values of ΔG and $T\Delta S$ were determined using equations $\Delta G = -RT\ln K$, and $T\Delta S = \Delta H - \Delta G$. All ITC profiles were fit to a model of single binding sites.

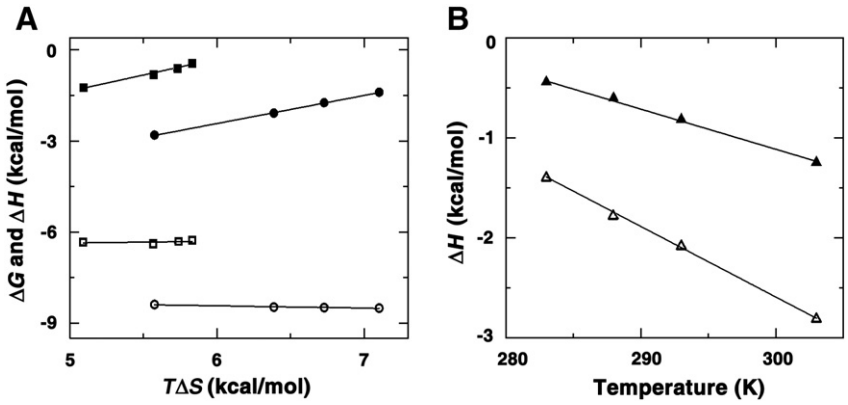

Fig. 7. (A) Plot of variation of ΔG (□,○) and ΔH (■,●) verses $T\Delta S$ for the binding of ADG and DAU with ss poly (A). (B) Plot of variation of enthalpy of binding (ΔH) with temperature for binding of ADG (▲) and DAU (△) with ss poly (A).

3.8. Absence of self-structure formation in ADG and DAU-poly(A) complexes

Self-structure formation is an important recently revealed aspect of many small molecule-poly(A) interactions [8,9,25,36,37,48]. One of our aims in this study was to investigate the capability of ADG and DAU in inducing self-structure in ss poly(A). Disappointingly, we found no evidence of any self-structure formation under a wide variety of solution conditions though many planar molecules that bind DNA by intercalation have been shown to induce it [25,36,48]. We feel that the presence of the additional sugar molecule in the chromophore may be the cause for the absence of the self-structure formation.

4. Conclusions

The present study compares the binding of two sugar containing antibiotics to single and double stranded poly(A) conformations. The binding has been studied by spectroscopy and calorimetry, enabling complete structural and thermodynamic characterization of the interaction. The results, both spectroscopic and calorimetry, revealed the highest affinity of DAU for ss and ds poly(A). ADG has lower binding affinities compared to DAU for both forms of poly(A). Results of ferrocyanide quenching studies suggested stacking and/or intercalation of these molecules into ss and ds poly(A), which is better with ss poly(A) for DAU and ds poly(A) for ADG. Calorimetric studies revealed that the binding is predominantly driven by large entropic contribution to the Gibbs energy, in particular for ss poly(A)-ADG and ds poly(A)-DAU. In all the cases non-polyelectrolytic force appears to be the major binding contribution in the complexation. There was no self-structure formation in ss poly(A) for both ADG and DAU indicating that the sugar moieties may be hindering such a conformational rearrangement.

Supplementary materials related to this article can be found online at doi:10.1016/j.bpc.2011.01.011.

Acknowledgements

This work was supported by grants from the network project on "*Comparative genomics and biology of noncoding RNA in the human genome*" (NWP0036) of the Council of Scientific and Industrial Research (CSIR), Government of India. Ms. Abhi Das is supported by the Junior Research Fellowship through NET of the CSIR. Dr. Kakali Bhadra was a Research Associate of the CSIR. Dr. Basudeb Achari was an Emeritus Scientist of CSIR. The authors thank Prof. Siddhartha Roy, Director, Indian Institute of Chemical Biology for his patronage. The help and cooperation of all the members of the Biophysical Chemistry Laboratory at every stage of this work are gratefully acknowledged. We also thank the anonymous reviewers for their critical and judicious comments that enabled us to improve upon the manuscript.

References

[1] P. Nelson, M. Kiriakidou, A. Sharma, E. Maniataki, Z. Mourelatos, The micro RNA world: small is mighty, Trends Biochem. Sci. 28 (2003) 534–540.
[2] C.C. Esau, B.P. Monia, Therapeutic potential for microRNAs, Adv. Drug Deliv. Rev. 59 (2007) 101–114.
[3] M.I. Zarudnaya, D.M. Hovorun, Structural transitions in polyadenylic acid and hypothesis on biological role of its double-stranded forms, Ukr. Biokhim. Zh. 71 (1999) 15–20.
[4] M.I. Zarudnaya, D.M. Hovorun, Hypothetical double-helical poly(A) formation in a cell and its possible biological significance, IUBMB Life 48 (1999) 581–584.
[5] S.M. Deev, N.I. Barbakar, A.V. Karlyshev, N.K. Sakharova, V.V. Grechko, Synthesis of double-stranded DNA on light immunoglobulin chain matrix RNA, Mol. Biol. (Mosk) 14 (1980) 413–420.
[6] U. Fuchs, A. Borkhardt, The application of siRNA technology to cancer biology discovery, Adv. Cancer Res. 96 (2007) 75–102.
[7] J.B. Harford, Translation-targeted therapeutics for viral diseases, Gene Expr. 4 (1995) 357–367.
[8] P. Giri, G. Suresh Kumar, Molecular recognition of poly(A) targeting by protoberberine alkaloids: in vitro biophysical studies and biological perspectives, Mol. Biosyst. 6 (2010) 81–88.
[9] P. Giri, G. Suresh Kumar, Molecular aspects of small molecules-poly(A) interaction: an approach to RNA based drug design, Curr. Med. Chem. 16 (2009) 965–987.
[10] M.J. Waring, DNA modification and cancer, Annu. Rev. Biochem. 50 (1981) 159–192.
[11] M.J. Waring, L.P.G. Wakelin, Echinomycin, a bifunctional intercalating antibiotic, Nature 252 (1974) 653–657.
[12] J.B. Chaires, Drug–DNA interactions, Curr. Opin. Struct. Biol. 8 (1998) 314–320.
[13] R. Martínez, L. Chacón-García, The search of DNA-intercalators as antitumoral drugs: what it worked and what did not work, Curr. Med. Chem. 12 (2005) 127–151.
[14] M. Maiti, G. Suresh Kumar, Molecular aspects on the interaction of protoberberine, benzophenanthridine, and aristolochia group of alkaloids with nucleic acid structure and biological perspectives, Med. Res. Rev. 27 (2007) 649–695.
[15] M. Maiti, G. Suresh Kumar, Protoberberine alkaloids: physicochemical and nucleic acid binding properties, top, Heterocycl. Chem. 10 (2007) 155–209.
[16] F. Walter, Q. Vicens, E. Westhof, Aminoglycoside–RNA interactions, Curr. Opin. Chem. Biol. 3 (1999) 694–704.
[17] Y. Qian, M.X. Guan, Interaction of aminoglycosides with human mitochondrial 12S rRNA carrying the deafness-associated mutation, Antimicrob. Agents Chemother. 53 (2009) 4612–4618.
[18] M.I. Recht, D. Fourmy, S.C. Blanchard, K.D. Dahlquist, J.D. Puglisi, RNA sequence determinants for aminoglycoside binding to an A-site rRNA model oligonucleotide, J. Mol. Biol. 262 (1996) 421–436.
[19] M.M. Islam, P. Pandya, S. Kumar, G. Suresh Kumar, RNA targeting through binding of small molecules: studies on t-RNA binding by the cytotoxic protoberberine alkaloid coralyne, Mol. Biosyst. 5 (2009) 244–254.
[20] M.M. Islam, G. Suresh Kumar, RNA targeting by small molecule alkaloids: studies on the binding of berberine and palmatine to polyribonucleotides and comparison to ethidium, J. Mol. Struct. 875 (2008) 382–391.
[21] Q. Vicens, E. Westhof, Molecular recognition of aminoglycoside antibiotics by ribosomal RNA and resistance enzymes: an analysis of X-ray crystal structures, Biopolymers 70 (2003) 42–57.
[22] H.F. Chambers, M.A. Chambers, in: Goodman and Gilman's The Pharmacological Basis of Theraputics, J.G. Hardman, L.E. Limbird, P.B. Molinoff, R.W. Ruddon, A.G. Gilman, (Eds.), ninth ed., McGraw-Hill, New York, 1996, ch. 46, pp. 1103–1121.

[23] P. Giri, M. Hossain, G. Suresh Kumar, Molecular aspects on the specific interaction of cytotoxic plant alkaloids palmatine to poly(A), Int. J. Biol. Macromol. 39 (2006) 210–221.
[24] P. Giri, M. Hossain, G. Suresh Kumar, RNA specific molecules: cytotoxic plant alkaloid palmatine binds strongly to poly(A), Bioorg. Med. Chem. Lett. 16 (2006) 2364–2368.
[25] P. Giri, G. Suresh Kumar, Self-structure induction in single stranded poly(A) by small molecules: studies on DNA intercalators, partial intercalators and groove binding molecules, Arch. Biochem. Biophys. 474 (2008) 183–192.
[26] P. Giri, G. Suresh Kumar, Binding of protoberberine alkaloid coralyne with double stranded poly(A): a biophysical study, Mol. Biosyst. 4 (2008) 341–348.
[27] R.C. Yadav, G. Suresh Kumar, K. Bhadra, P. Giri, R. Sinha, S. Pal, M. Maiti, Berberine, a strong polyriboadenylic acid binding plant alkaloid: spectroscopic, viscometric, and thermodynamic study, Bioorg. Med. Chem. 13 (2005) 165–174.
[28] P. Giri, G. Suresh Kumar, Spectroscopic and calorimetric studies on the binding of the phototoxic and cytotoxic plant alkaloid sanguinarine with double helical poly (A), J. Photochem. Photobiol. A Chem. 194 (2008) 111–121.
[29] M. Wickens, P. Anderson, R.J. Jackson, Life and death in the cytoplasma: messages from the 3′ end, Curr. Opin. Genet. Dev. 7 (1997) 220–232.
[30] K. Dower, N. Kuperwasser, H. Merrikh, M. Rosbash, A synthetic tail rescues yeast nuclear accumulation of ribozyme-terminated transcript, RNA 10 (2004) 1888–1899.
[31] S.L. Topalian, S. Kaneko, M.I. Gonzales, G.L. Bond, Y. Ward, J.L. Manley, Identification and functional characterization of neo-Poly(A) polymerase, an RNA processing enzyme overexpressed in human tumors, Mol. Cell. Biol. 21 (2001) 5614–5623.
[32] S.L. Topalian, M.I. Gonzales, Y. Ward, X. Wang, R.F. Wang, Revelation of a cryptic major histocompatibility complex class II-restricted tumor epitope in a novel RNA processing enzyme, Cancer Res. 62 (2002) 5505–5509.
[33] W. Saenger, Principles of Nucleic Acid Structure, Springer-Verlag, New York, 1984.
[34] A.G. Petrovic, P.L. Polavarapu, Structural transitions in polyriboadenylic acid induced by the changes in pH and temperature: vibrational circular dichroism study in solution and film states, J. Phys. Chem. B 109 (2005) 23698–23705.
[35] W.M. Scovell, Structural and conformational studies of polyriboadenylic acid in neutral and acid solution, Biopolymers 17 (1978) 969–984.
[36] F. Xing, G. Song, J. Ren, J.B. Chaires, X. Qu, Molecular recognition of nucleic acids: coralyne binds strongly to poly(A), FEBS Lett. 579 (2005) 5035–5039.
[37] H. Xi, D. Grey, S. Kumar, D.P. Arya, Molecular recognition of single stranded RNA: neomycin binding to poly(A), FEBS Lett. 583 (2009) 2269–2275.
[38] C. Ciatto, M.L. D'Amico, G. Natile, F. Secco, M. Venturini, Intercalation of proflavine and a platinum derivative of proflavine into double-helical Poly(A), Biophys. J. 77 (1999) 2717–2724.
[39] S.C. Pakrashi, P. Ghosh-Dastidar, S. Basu, B. Achari, New phenanthrene derivatives from *Aristolochia indica*, Phytochemical 16 (1977) 1103–1104.
[40] B. Achari, S. Bandyopadhyay, A.K. Chakraborty, S.C. Pakrashi, Carbon-13 NMR spectra of some phenanthrene derivatives from Aristolochia indica and their analogues, Org. Mag. Reson. 22 (1984) 741–746.
[41] K. Bhadra, G. Suresh Kumar, S. Das, M.M. Islam, M. Maiti, Protonated structures of naturally occurring deoxyribonucleic acids and their interaction with berberine, Bioorg. Med. Chem. 13 (2005) 4851–4863.
[42] J.D. McGhee, P.H. von Hippel, Theoretical aspects of DNA–protein interactions: cooperative and noncooperative binding of large ligands to a one dimensional homogeneous lattice, J. Mol. Biol. 86 (1974) 469–489.
[43] H.A. Benesi, J.H. Hildebrand, A spectrophotometric investigation of the interaction of iodine with aromatic hydrocarbons, J. Am. Chem. Soc. 71 (1949) 2703–2707.
[44] S.M. Hoenigman, C.E. Evans, Improved accuracy and precision in the determination of association constants, Anal. Chem. 68 (1996) 3274–3276.
[45] R. Sinha, M.M. Islam, K. Bhadra, G. Suresh Kumar, A. Banerjee, M. Maiti, The binding of DNA intercalating and non-intercalating compounds to A-form and protonated form of poly(rC).poly(rG): spectroscopic and viscometric study, Bioorg. Med. Chem. 14 (2006) 800–814.
[46] P. Job, Formation and stability of inorganic complexes in solution, Ann. Chim. 9 (1928) 113–203.
[47] C.Y. Huang, in: S.P. Colowick, N.O. Kaplan (Eds.), Determination of Binding Stoichiometry by the Continuous Variation Method: The Job Plot, Methods Enzymol., 87, Academic Press, 1982, pp. 509–525.
[48] P. Giri, G. Suresh Kumar, Specific binding and self-structure induction to poly(A) by the cytotoxic plant alkaloid sanguinarine, Biochim. Biophys. Acta 1770 (2007) 1419–1426.
[49] M.M. Islam, R. Sinha, G. Suresh Kumar, RNA binding small molecules: studies on t-RNA binding by cytotoxic plant alkaloids berberine, palmatine and the comparison to ethidium, Biophys. Chem. 125 (2007) 508–520.
[50] K. Bhadra, M. Maiti, G. Suresh Kumar, Molecular recognition of DNA by small molecules: AT base pair specific intercalative binding of cytotoxic plant alkaloid palmatine, Biochim. Biophys. Acta 1770 (2007) 1071–1080.
[51] S. Das, G. Suresh Kumar, Molecular aspects on the interaction of phenosafranine to deoxyribonucleic acid: model for intercalative drug–DNA binding, J. Mol. Struct. 872 (2008) 56–63.
[52] J.R. Lakowicz, Principles of Fluorescence Spectroscopy, first ed.Plenum Press, New York, 1983.
[53] N.J. Buurma, I. Haq, Advance in the analysis of isothermal titration calorimetry data for ligand–DNA interactions, Methods 42 (2007) 162–172.
[54] A.L. Faig, Applications of isothermal titration calorimetry in RNA biochemistry and biophysics, Biopolymers 87 (2007) 293–301.
[55] K. Bhadra, G. Suresh Kumar, Isoquinoline alkaloids and their binding with DNA: calorimetry and thermal analysis applications, Mini Rev. Med. Chem. 10 (2010) 1235–1247.
[56] J.B. Chaires, Biophysical chemistry of the daunomycin–DNA interaction, Biophys. Chem. 35 (1990) 191–202.
[57] S. Chakraborty, R. Nandi, M. Maiti, Thermodynamics of the interaction of aristololactam-β-D-glucoside with DNA, Biochem. Pharmacol. 39 (1990) 1181–1186.
[58] J.B. Chaires, Energetics of drug–DNA interactions, Biopolymers 44 (1997) 201–215.
[59] J. Ren, T.C. Jenkins, J.B. Chaires, Energetics of DNA intercalation reactions, Biochemistry 39 (2000) 8439–8447.
[60] P.H. Lin, Y.H. Kao, Y. Chang, Y.C. Cheng, C.C. Chien, W.Y. Chen, Daunomycin interaction with DNA: microcalorimetric studies of the thermodynamics and binding mechanism, Biotechnol. J. 5 (2010) 1069–1077.